A Developed ESPRIT for Moving Target 2D-DOAE

Youssef Fayad, Member, IAENG, Caiyun Wang, and Qunsheng Cao

***Abstract*— In this paper a modified ESPRIT algorithm, which bases on a time subspace concept (T-ESPRIT) to estimate 2D-DOA (azimuth and elevation) of a radiated source, that can increase the estimation accuracy with low computational load is introduced. Moreover, in order to upgrade the estimation accuracy, the DOAE is corrected with Doppler frequency (f_d) which induced by target movement. The efficacy of the proposed algorithm is verified by using the Monte Carlo simulation; the DOAE accuracy has been evaluated by the closed-form Cramér–Rao bound (CRB). The proposed algorithm shows the estimated results better than those of the normal ESPRIT methods improving the estimator performance.**

***Index Terms*— DOAE, Subspace, ESPRIT, Doppler Effect.**

I. Introduction

Estimating of direction-of-arrival (DOAE) is a very important process in radar signal processing applications. DOAE is the creator of the tracking gate dimensions (the azimuth and the elevation) in the tracking while scan radars (TWS). Accurate DOAE leads to reduce the angle glint error which affects the accuracy of the tracking radars. The ESPRIT and its extracts have been widely studied in one-dimensional (1D) DOAE for uniform linear array (ULA), non-uniform linear array (NULA) [1]-[11], and also extended to two-dimensional (2D) DOAE [12]-[20]. All of these ESPRIT methods have been developed to upgrade the accuracy of estimation or decrease the calculation costs. The main challenge facing these methods is the high computational load for more DOAE accuracy. Furthermore, these works did not study the effect of the Doppler frequency on the DOAE accuracy.

This paper presents a new modified algorithm based on time subspace (T-ESPRIT) [1], [2] to estimate the 2D-DOA in a co-located planar array. T-ESPRIT method reduces the model non-linearity effect by picking the data points enclosed by each snapshot. It also reduces the computational load via processing the temporal subspaces in parallel which leads to shrink the covariance matrix dimension.

Manuscript received May 27, 2015. This work was supported in part by the Key Laboratory of Radar Imaging and Microwave Photonics (Nanjing University of Aeronaut and Astronaut.), Ministry of Education, Nanjing University of Aeronautics and Astronautics, Nanjing, China.

Youssef Fayad. Author is with the College of Electronic and Information Engineering, Nanjing University of Aeronautics& Astronautics, Nanjing 210016, China (corresponding author to provide phone: 008618351005349; e-mail: youssefyad595@yahoo.com; youssefyad@nuaa.edu.cn).

Caiyun Wang. Author is with the College of Astronautics, Nanjing University of Aeronautics& Astronautics, Nanjing 210016, China (e-mail: wangcaiyun@nuaa.edu.cn).

Qunsheng Cao. Author is with the College of Electronic and Information Engineering, Nanjing University of Aeronautics& Astronautics, Nanjing 210016, China (e-mail:qunsheng @nuaa.edu.cn).

Finally, the effect of Doppler frequency on the T-ESPRIT method has been derived in order to reduce the effect of target maneuver on the DOAE accuracy, which consequently reduces the target trajectory estimation errors and improves the radar angular resolution. Thus, the proposed method enhances the estimation accuracy and reduces computational complexity [21], [22].

The reminder of the paper is organized as follows. In Section II, the 2D T-ESPRIT DOAE technique has been introduced and the Doppler Effect on DOAE process has been derived. The simulation results are presented in section III. And section IV is conclusions.

II. Proposed Algorithm

A. The Measurement Model

In this model, the transmission medium is assumed to be isotropic and non-dispersive, so that the radiation propagates in straight lines, and the sources are assumed as a far-field away the array. Consequently, the radiation impinging on the array is a summation of the plane waves. The signals are assumed to be narrow-band processes, and they can be considered to be sample functions of a stationary stochastic process or deterministic functions of time. Considering there are K narrow-band signals, and the center frequency (ω_0) is assumed to be the same, for the k^{th} signal can be written as,

$$s_k(t) = E_k e^{j(\omega_0 t+\Psi_k)}, k = 1, 2, \dots, \mathrm{K} \quad (1)$$

where, $s_k(t)$ is the signal of the k^{th} emitting source at time instant t, Ψ_k is the carrier phase angles are assumed to be random variables, each uniformly distributed on $[0,2\pi]$ and all statistically independent of each other, and E_k is the incident electric field, can be written as components form. As a general expression, we omit the subscript, then

$$\vec{E} = E_\theta \hat{e}_\theta + E_\varphi \hat{e}_\varphi \quad (2)$$

where E_φ and E_θ are the horizontal and the vertical components of the field, respectively.

Defining $\gamma \in [0, \pi/2]$ as the auxiliary polarization angle, $\eta \in [-\pi, \pi]$ as the polarization phase difference, then,

$$E_\varphi = |\vec{E}| \cos\gamma,\ E_\theta = |\vec{E}| \sin\gamma e^{j\eta}. \quad (3)$$

The incident field can be also expressed in Cartesian coordinate system,

$$\vec{E} = E_\theta \hat{e}_\theta + E_\varphi \hat{e}_\varphi = \left(E_\theta \cos\theta \cos\varphi - E_\varphi \sin\varphi\right)\hat{e}_x + \left(E_\theta \cos\theta \sin\varphi + E_\varphi \cos\varphi\right)\hat{e}_y + (E_\theta \sin\theta)\hat{e}_z \quad (4)$$

Fig. 1 shows a planar antenna array has elements indexed *L*, *I* along *y* and *x* directions, respectively. For any pairs (*i*, *l*), its coordinate is (*x*, *y*) = ((*i*-1) Δ_x, (*l*-1) Δ_y), where *i=1,…,I, l=1,…,L*, Δ_x and Δ_y are reference displacements between neighbor elements along *x* and *y* axis. The array elements are oriented in *xoy* plane, the space phase factors along *x* and *y* directions are expressed as,

$$p_i(\theta_k, \varphi_k) \equiv p_i^k = e^{j\frac{2\pi(i-1)\Delta_x}{\lambda} \sin\theta_k \cos\varphi_k} \quad (5a)$$

$$q_l(\theta_k, \varphi_k) \equiv q_l^k = e^{j\frac{2\pi(l-1)\Delta_y}{\lambda} \sin\theta_k \sin\varphi_k} \quad (5b)$$

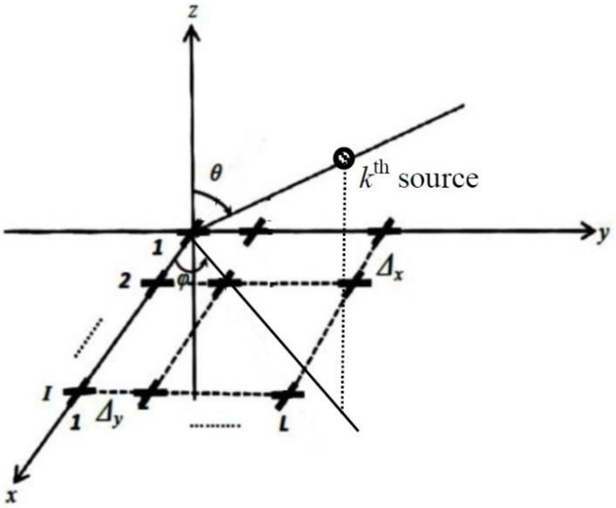

Fig. 1 Planar antenna array

where, (θ_k, φ_k) denote the k^{th} source elevation angle and azimuth angle respectively, and λ is the wavelength of the k^{th} signal. The measurement vector can be expressed as,

$$z_{i,l}(t) = \sum_{k=1}^{K} u_k s_k(t) p_i(\theta_k, \varphi_k) q_l(\theta_k, \varphi_k) + w_{i,l}(t) \quad (6a)$$

$$[Z(t)] = \left[z_{1,1}(t) \ \cdots \ z_{1,L}(t) \ \cdots \ z_{I,1}(t) \ \cdots \ z_{I,L}(t)\right]^T \quad (6b)$$

where $[W(t)]$ stands for the additive white Gaussian noise (AWGN), it is consisted as,

$$[W(t)] = \left[w_{1,1}(t) \ \cdots \ w_{1,L}(t) \ \cdots \ w_{I,1}(t) \ \cdots \ w_{I,L}(t)\right]^T \quad (7)$$

From (3) and (4), we got

$$u_k = \begin{pmatrix} \sin\gamma_k \cos\theta_k \cos\varphi_k \, e^{j\eta_k} - \cos\gamma_k \sin\varphi_k \\ \sin\gamma_k \cos\theta_k \sin\varphi_k e^{j\eta_k} + \cos\gamma_k \cos\varphi_k \end{pmatrix} \quad (8)$$

For receiving array, the whole receiving factors in subspaces matrix are included in $[a(\theta_k, \varphi_k)]$ that is,

$$a(\theta_k, \varphi_k) \stackrel{\text{def}}{=} p(\theta_k, \varphi_k) \otimes q(\theta_k, \varphi_k) \quad (9)$$

where $\otimes$ denotes the Kronker product, so

$$A(\theta_k, \varphi_k) = [u_k^T p_1^k q_1^k \ u_k^T p_1^k q_2^k \ldots u_k^T p_1^k q_L^k \ \ u_k^T p_2^k q_1^k \ \ u_k^T p_2^k q_2^k \cdots u_k^T p_2^k q_L^k$$

$$\cdots u_k^T p_I^k q_1^k \ u_k^T p_I^k q_2^k \cdots u_k^T p_I^k q_L^k]^T \quad (10)$$

The receiving model can be rewritten as,

$$[Z(t)] = [A] S(t) + [W(t)] \quad (11)$$

where $S(t) \stackrel{\text{def}}{=} [s_1(t) \ \cdots \ \ \cdots \ s_K(t)]^T$

and, $[A] \stackrel{\text{def}}{=} \left[A(\theta_1\varphi_1) \ \cdots \ \ \cdots \ A(\theta_K, \varphi_K)\right]$

The subspace approach not only decreases the computational load as a result of shrinking the matrix dimensions, but it also reduces the influence of non-linearity when deals with signal inside each small time step as a linear part.

For the electronic scanning beam (ESB) with width W_{az} scans β sector; the dwell interval T_D is obtained as follows [23],

$$T_D = \frac{W_{az} \times 60}{\beta \times \vartheta} \quad (12)$$

where ϑ is the number of scans per minute,

$$Number\ of\ hits = T_D \times PRF \quad (13)$$

where *PRF* is the pulse repetition frequency.

Using the T-ESPRIT method, the whole data is divided into *M* snapshots each shares *T* seconds. Then, it picks up enough *r* data points enclosed by each snapshot *m* with time period $\tau = \frac{T}{r}$ as short as possible. So, from (11) each receiving signal measurement value through m^{th} subspace is given as,

$$[z^m(\tau)] = [A] s^m(\tau) + [w^m(\tau)] \quad (14)$$

The index *m* runs as *m* =1, 2, …, *M* snapshots. Therefore, the whole data matrix can be expressed as,

$$\mathbf{Z} \stackrel{\text{def}}{=} \begin{bmatrix} z_{1,1}^1(0) & \ldots & z_{1,1}^1(\tau_1) \ldots \ldots z_{1,1}^m(0) & \ldots & z_{1,1}^m(\tau_1) \ldots \ldots z_{1,1}^M(0) & \ldots & z_{1,1}^M(\tau_1) \\ \vdots & \ddots & \vdots \quad\quad \vdots & \ddots & \vdots \quad\quad \vdots & \ddots & \vdots \\ z_{I,L}^1(0) & \ldots & z_{I,L}^1(\tau_1) \ldots \ldots z_{I,L}^m(0) & \ldots & z_{I,L}^m(\tau_1) \ldots \ldots z_{I,L}^M(0) & \ldots & z_{I,L}^M(\tau_1) \end{bmatrix} \quad (15)$$

where, $\tau_1 = (r-1) \times \tau$.

The dimension of [Z] for the k^{th} signal is 2(*I*·*L*·*Mr*). For the m^{th} subspace data matrix can be expressed as,

$$[z^m(\tau)] = \begin{bmatrix} z_{1,1}^m(0) & \ldots & z_{1,1}^m(\tau_1) \\ \vdots & \ddots & \vdots \\ z_{I,L}^m(0) & \ldots & z_{I,L}^m(\tau_1) \end{bmatrix} \quad (16)$$

For T-ESPRIT scheme, the ESPRIT algorithm is used in an appropriate picked data represented in (15) for each (*m*) subspace - shown in (16) - in parallel for the same sampling accuracy thus reducing the calculations load and consequently saving time is achieved. Fig. 2 is the time baseline and the time series which indicates the subspace approach. Fig. 3 is given the diagram of a 2D T-ESPRIT method.

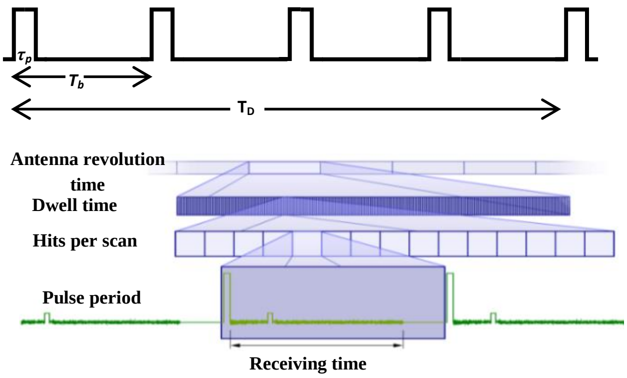

(a)

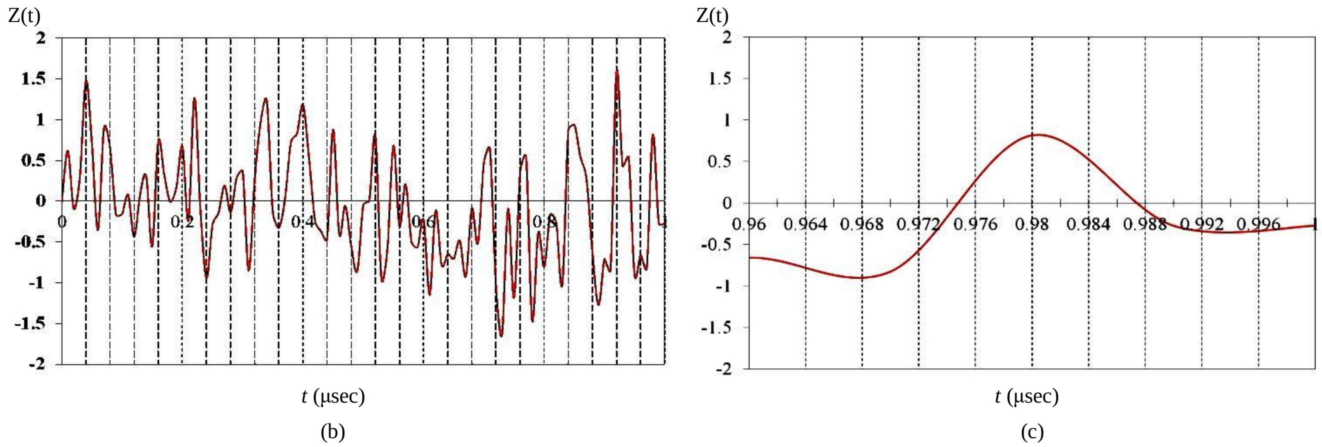

Fig. 2 (a) Time- baseline, (b) total signal in time series, (c) signal in 25th snapshot.

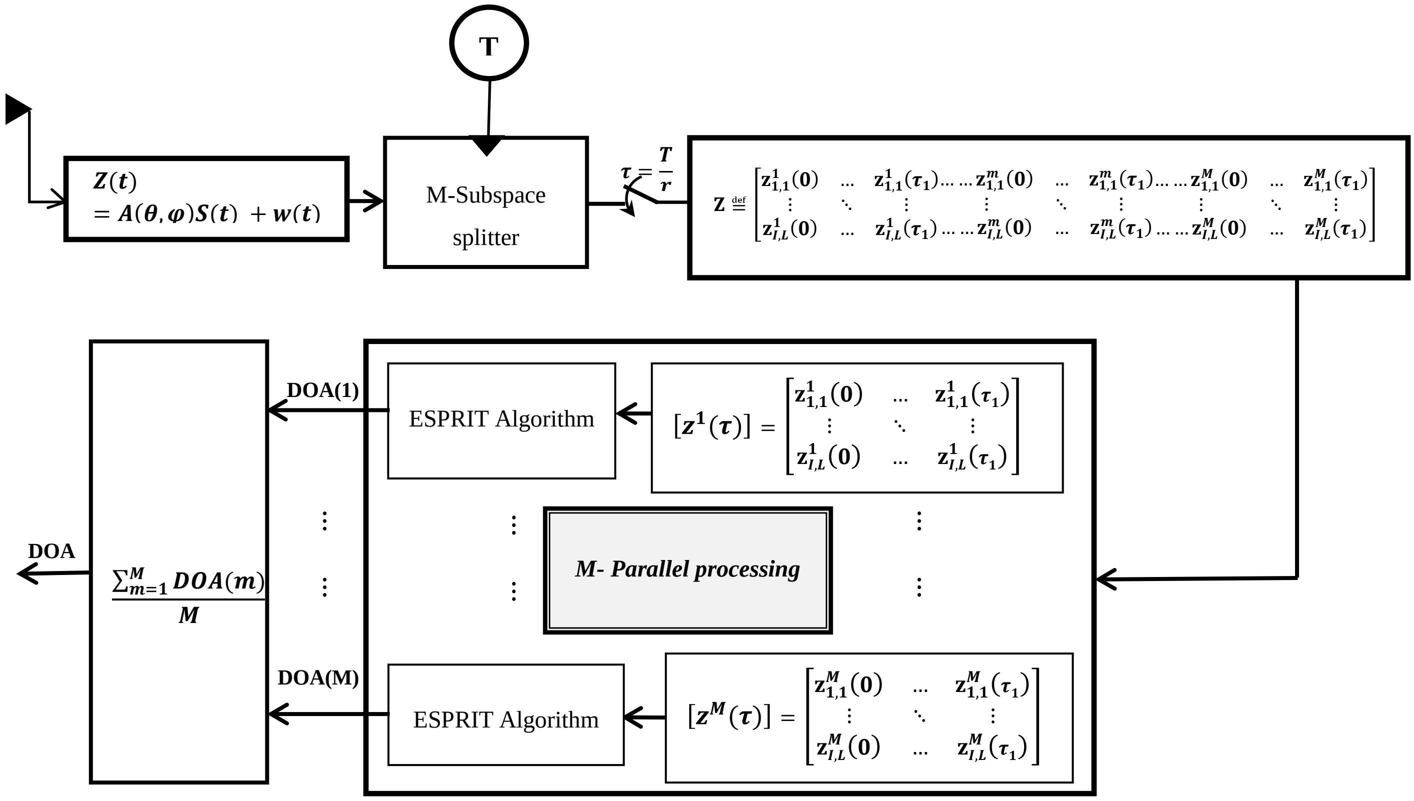

Fig. 3 Planar Array T-ESPRIT Technique

As shown in Fig.2 (a) and from (12), (13), the TWS radar with 4 hits, τ_p=0.25 μsec, and T_b =250 μsec has $T_D = 1$ msec. Moreover, after the radar pulse integration [24] the total signal time is 1 μsec. according to the Nyquist law the whole signal is divided to M =25 snapshots as shown in Fig.2 (b), and each shares $T = 0.04$ μsec, then it picks up data points enclosed by each snapshot with time period $\tau = 0.002$ μsec as shown in Fig.2 (c).

B. T-ESPRIT method for 2-D DOAE

The ESPRIT algorithm is based on a covariance formulation that is,

$$\hat{R}_{zz} \stackrel{\text{def}}{=} E[Z(\tau)Z(\tau)^H] = A\hat{R}_{ss}A^H + \sigma^2\Sigma_w \tag{17}$$

$$\hat{R}_{ss} = E[S(\tau)S^H(\tau)] \tag{18}$$

where $\hat{R}_{zz}$ is the correlation matrix of the array output signal matrix, $\hat{R}_{ss}$ is the autocorrelation matrix of the signal. The subscript H denotes the complex conjugate transpose.

The correlation matrix of $\hat{R}_{zz}$ can be done for eigenvalue decomposition as follows,

$$\hat{R}_{zz} \stackrel{\text{def}}{=} \hat{E}_S \Lambda \hat{E}_S^H + \sigma^2 \hat{E}_N \Lambda \hat{E}_N^H \quad (19)$$

Where the eigenvalues are ordered,
$\lambda_1 > \lambda_2 > \cdots > \lambda_K > \cdots \lambda_{2(I\times L)}$, $\lambda_{K+1} = \cdots = \lambda_{2(I\times L)} = \sigma^2$.

The eigenvectors $\hat{E}_S = [\hat{e}_1, \hat{e}_2, \cdots, \hat{e}_K]$ for largest K eigenvalues spans the signal subspace, the rest $2(I\times L) - K$ smallest eigenvalues $\hat{E}_N = [\hat{e}_{K+1}, \cdots, \hat{e}_{2(I\times L)}]$ spans the noise subspace which is orthogonal to the signal subspace. Therefore, there exists a unique nonsingular matrix Q, such that,

$$\hat{E}_S = [A]Q = [u_k^T \otimes p_i(\theta_k, \varphi_k) \otimes q_l(\theta_k, \varphi_k)]Q \quad (20)$$

In (10) let A_{P1} and A_{P2} be the first and the last $2L\times(I-1)$ rows of A respectively, they differ by the factor $\Delta p_k = e^{j\frac{2\pi\Delta_x}{\lambda}\sin\theta_k\cos\varphi_k}$ along the x direction. So $A_{P2} = A_{P1}\emptyset_P$, where $\emptyset_P$ is the diagonal matrix with diagonal elements Δp_k. Consequently, $\hat{E}_{P1}$ and $\hat{E}_{P2}$ will be the first and the last $2L\times(I\text{-}1)$ sub-matrices formed from $\hat{E}_S$. Then the diagonal elements p_k of $\emptyset_P$ are the eigenvalues of the unique matrix $\Psi_P = Q^{-1}\emptyset_P Q$, that satisfies,

$$\hat{E}_{P2} = \hat{E}_{P1}\Psi_P. \quad (21)$$

Similarly, the two $2I\times(L\text{-}1)$ sub-matrices A_{q1} and A_{q2} consist of the rows of A numbered $2L\times(i-1)+l$ and $2L\times(i-1)+l+2$ respectively, differ by the space factors $\Delta q_k = e^{j\frac{2\pi\Delta_y}{\lambda}\sin\theta_k\sin\varphi_k}$ along the y direction, *l=1,...,2(L-1)*. Then $A_{q2} = A_{q1}\emptyset_q$ where $\emptyset_q$ is the diagonal matrix with diagonal elements Δq_k. Consequently, $\hat{E}_S$ forms the $2I\times(L\text{-}1)$ two sub-matrices $\hat{E}_{q1}$ and $\hat{E}_{q2}$. Then the diagonal elements Δq_k of $\emptyset_q$, are the eigenvalues of the unique matrix $\Psi_q = Q^{-1}\emptyset_q Q$, that satisfies,

$$\hat{E}_{q2} = \hat{E}_{q1}\Psi_q \quad (22)$$

Therefore, the arrival angles (θ_k, φ_k) can be calculated as:

$$\theta_k = sin^{-1}\left\{\frac{\lambda}{2\pi}\left[\left(\frac{arg(\Delta p_k)}{\Delta_x}\right)^2 + \left(\frac{arg(\Delta q_k)}{\Delta_y}\right)^2\right]^{1/2}\right\} \quad (23)$$

$$\varphi_k = tan^{-1}\left[\frac{\Delta_x}{\Delta_y}\cdot\frac{arg(q_k)}{arg(p_k)}\right] \quad (24)$$

C. Doppler frequency effect on the estimation process

The moving target echo signal is shifted by the Doppler Effect. The more accurate T-ESPRIT algorithm should consider the effect of the Doppler frequency shift due to the target movement. So for the co-located planar array,

$$arg(\Delta p_k) = \frac{2\pi}{\grave{\lambda}_x}\Delta_x \sin\theta_k \cos\varphi_k \quad (25)$$

$$arg(\Delta q_k) = \frac{2\pi}{\grave{\lambda}_y}\Delta_y \sin\theta_k \sin\varphi_k \quad (26)$$

where $\grave{\lambda}_x$ and $\grave{\lambda}_y$ are the wavelength components of the received wave into antenna plane and differ from the transmitted wavelength because of the Doppler frequency f_d caused by the target moving velocity $\vec{v}_s$ [25], [26], [27].
As shown in Fig. 4, it is obvious that the wavelength $\grave{\lambda}_x$ and $\grave{\lambda}_y$ have expressions caused by the velocity components v_x and v_y,

$$\grave{\lambda}_x = \frac{\lambda(c+v_x)}{c} \quad (27)$$

$$\grave{\lambda}_y = \frac{\lambda(c+v_y)}{c} \quad (28)$$

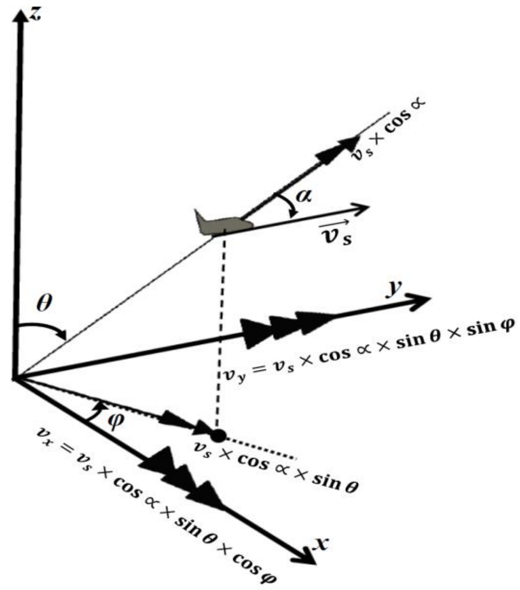

Fig. 4 Target linear velocity components into antenna plane

Substituting into (23)-(24), then,

$$arg(\Delta p_k) = \frac{2\pi c}{\lambda(c+v_x)}\Delta_x \sin\theta_k \cos\varphi_k \quad (29)$$

$$arg(\Delta q_k) = \frac{2\pi c}{\lambda(c+v_y)}\Delta_y \sin\theta_k \sin\varphi_k \quad (30)$$

where,

$$v_x = |\vec{v}_s| \cos\alpha \sin\theta_k \cos\varphi_k \quad (31)$$

$$v_y = |\vec{v}_s| \cos\alpha \sin\theta_k \sin\varphi_k \quad (32)$$

And,

$$|\vec{v}_s| = \frac{c\cdot f_d}{2f\cdot\cos\alpha} \quad (33)$$

where α is defined as the angle between the direction of propagation and the target velocity vector $\vec{v}_s$, the value of α changes f_d sign indicating the target direction toward or away from the antenna position. From (29)-(32) the arrival angles (θ_k, φ_k) can be fine estimated from $(arg(p_k), arg(q_k))$ as follows,

$$\theta_k = sin^{-1}\left\{\left[\left(\frac{c\cdot arg(\Delta p_k)}{(2\pi c\Delta_x/\lambda) - arg(\Delta p_k)\cdot|\vec{v}_s|\cos\alpha}\right)^2 + \left(\frac{c\cdot arg(\Delta q_k)}{(2\pi c\Delta_y/\lambda) - (arg(\Delta q_k)\cdot|\vec{v}_s|\cos\alpha}\right)^2\right]^{1/2}\right\} \quad (34)$$

$$\varphi_k = tan^{-1}\left[\frac{arg(\Delta q_k)}{arg(\Delta p_k)} \cdot \frac{(2\pi c\Delta_x/\lambda) - arg(\Delta p_k)\cdot|\vec{v}_s|\cos\alpha)}{(2\pi c\Delta_y/\lambda) - arg(\Delta q_k)\cdot|\vec{v}_s|\cos\alpha}\right] \quad (35)$$

It is obviously found from (34), (35) that if $\vec{v}_s = 0$, it will realize for a stationary target indicated in (23), (24).

III. CRAMÉR–RAO BOUNDS (CRB) FOR THE 2D CASE

The Cramér–Rao bound has provided more accuracy achievable by any unbiased estimator of signal parameters and fundamental physical limit on system accuracy [28], [29]. For Gaussian process, M snapshots, and response $A(\theta,\varphi)$ corresponding sensors I×L, it has,

$$P(Z/(\theta,\varphi)) = \frac{1}{\sqrt{2\pi\delta^2}} e^{\frac{\sum_{m=1}^{M} -(Z_m - S_m A(\theta,\varphi))(Z_m - S_m A(\theta,\varphi))^T}{2\delta^2}} \qquad (36)$$

Substitute with

$$F_m = Z_m - S_m A(\theta,\varphi) \qquad (37)$$

Then we have,

$$\ln P(Z|(\theta,\varphi)) = \ln\frac{1}{\sqrt{2\pi\delta^2}} - \frac{1}{2\delta^2}\sum_{m=1}^{M}(F_m)(F_m)^T \qquad (38)$$

To get the CRB we first calculate $E\left[\frac{\partial^2 \ln P(Z/(\theta,\varphi))}{\partial\theta\,\partial\varphi}\right]$, which denotes the expected value (sample mean)

$$E\left[\frac{\partial^2 \ln P(Z/(\theta,\varphi))}{\partial\theta\,\partial\varphi}\right] = -\frac{M}{\sigma^2}\cdot E\left[\begin{pmatrix} \frac{\partial^2 J}{\partial\theta^2} & \frac{\partial^2 J}{\partial\theta\partial\varphi} \\ \frac{\partial^2 J}{\partial\varphi\partial\theta} & \frac{\partial^2 J}{\partial\varphi^2} \end{pmatrix}\right] \qquad (39)$$

where $J = \frac{1}{2}F_m F_m^T$.

For simplicity let F_m denoted by F,

$$\frac{\partial J}{\partial\theta} = \frac{\partial J}{\partial F}\frac{\partial F}{\partial\theta} + \frac{\partial J}{\partial F^T}\frac{\partial F^T}{\partial\theta},\ \frac{\partial J}{\partial\varphi} = \frac{\partial J}{\partial F}\frac{\partial F}{\partial\varphi} + \frac{\partial J}{\partial F^T}\frac{\partial F^T}{\partial\varphi} \qquad (40)$$

$$FIM = -E\left[\frac{\partial^2 \ln P(Z|(\theta,\varphi))}{\partial\theta\,\partial\varphi}\right] \qquad (41)$$

Where FIM expresses the Fisher Information Matrix. Substitute from (37), (40) then into (39) and (41), we got,

$$FIM = 2M\left(\frac{S}{\delta}\right)^2 Real\begin{bmatrix} \frac{\partial(A^T(\theta,\varphi))}{\partial\theta}\frac{\partial(A(\theta,\varphi))}{\partial\theta} & \frac{\partial(A^T(\theta,\varphi))}{\partial\varphi}\frac{\partial(A(\theta,\varphi))}{\partial\theta} \\ \frac{\partial(A^T(\theta,\varphi))}{\partial\theta}\frac{\partial(A(\theta,\varphi))}{\partial\varphi} & \frac{\partial(A^T(\theta,\varphi))}{\partial\varphi}\frac{\partial(A(\theta,\varphi))}{\partial\varphi} \end{bmatrix} \qquad (42)$$

Finally, we have,

$$CRB = [FIM]^{-1} \qquad (43)$$

IV. SIMULATION RESULTS

Considering the 2D-DOAE process with AWGN, the parameters are given T_D=1msec, $\beta = 90°$, $W_{az} = 1.5°$, number of hits = 4, $\vartheta = 1000$ scan/min, number of hits = 4, $v_s = 250\ m/sec$, $f = 3\ GHz$, $\alpha = 0°$ (f_d= 5000Hz), and f_s = 25 MHz. Assuming total 25 temporal snapshots, pickup enclosed data r =20 times, 200 independent Monte Carlo simulations, and SNR = -5 to15dB. In order to validate the T-ESPRIT method, it has used in the planar case with different number of elements, such as (I, L) = (5, 5) and (6, 6) with displacement values $\Delta_x = \Delta_y = \lambda/2$, with θ=45° and φ=60°. Figs. 5 (a) and (b) are depicted the subspace DOAE process. It is found that the computational load was reduced as a result of reducing the measurement matrix dimension to $(2IL \times r)$ instead of $(2IL \times Mr)$ and employ the subspaces parallel processing concept. Table I represents the computational time and complexity of the proposed method in term of number of flip-flops. It is obvious that the computational load has been reduced as a result of applying the ESPRIT algorithm on the captured r data for each m subspace $[z^m(\tau)]_{(2IL\times r)}$in parallel. It gives us a simultaneous processing for M subspaces with each has r snapshots instead of processing for one space has a large number of snapshots d, (d=Mr) snapshots.

TABLE I
Comparison of the required computation time and complexity

Algorithm / computational	Conventional ESPRIT	Proposed algorithm
time (msec)	16.78	1.62
complexity	$O(4d(IL)^2+ 8(IL)^3)$	$O(M+4r(IL)^2+8(IL)^3)$

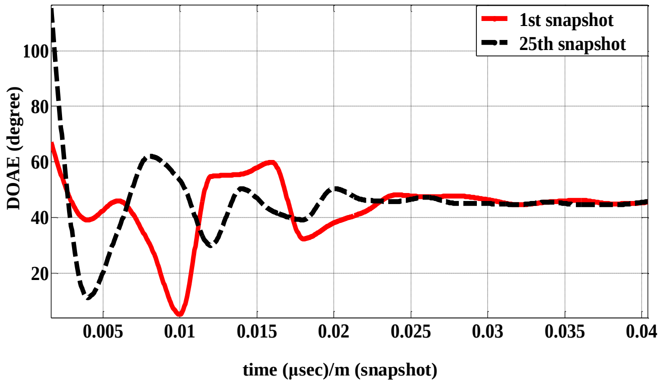

(a)

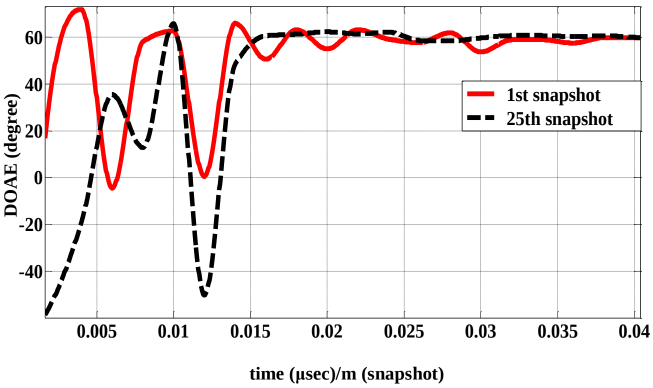

(b)

Fig. 5 Implementation of the T-ESPRIT method for the PA for $\Delta_x = \Delta_y = \lambda/2$, (a) θ=45°, (b) φ=60°

Figs. 6 (a, b) are plotted the T-ESPRIT RMSEs with different number of elements. The T-ESPRIT RMSEs with the Doppler correction for the same conditions is depicted in Fig. 6(b). Results in Fig. 6 (a) indicate that the T-ESPRIT errors are getting closer to the CRB due to increase the number of elements. Fig. 6 (b) indicates that the accuracy is upgraded by taking the Doppler Effect into account which decreases effectively the estimation errors and enables a high DOAE accuracy with fewer numbers of elements.

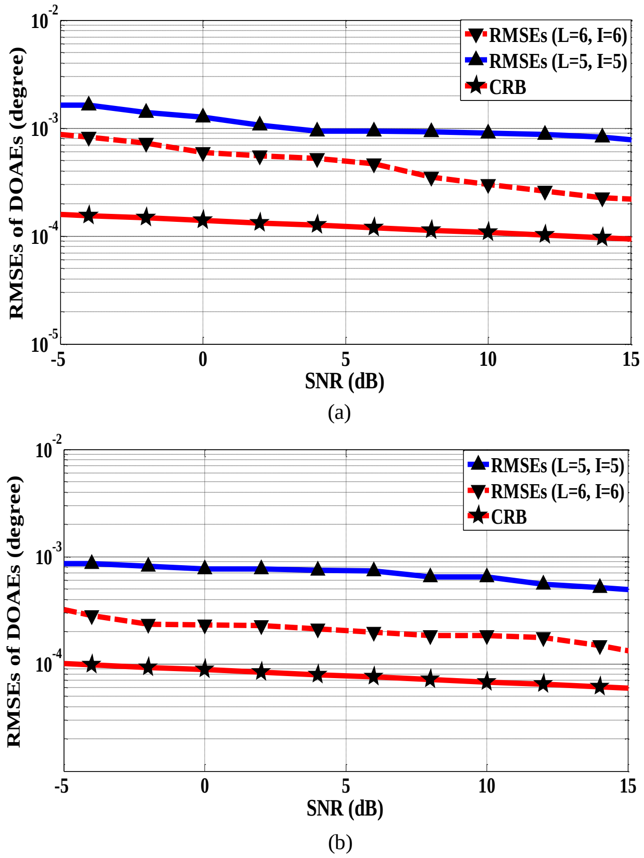

Fig. 6 The RMSEs of T-ESPRIT method for PA with different number of elements for Δx= Δy=λ/2, at θ=45°, φ=60°, (a) without; (b) with Doppler correction.

The accuracy improvement of the 2D-DOAE using proposed algorithm has been verified by comparing the resulted RMSEs with the RMSEs of different ESPRIT algorithms used in [15], [17], and [20]. Fig. 7 shows comparison between the proposed algorithm errors and errors of the 2D Beam ESPRIT, the ESPRIT-Like, and the Quaternion ESPRIT algorithms used in [15], [17], and [20] respectively.

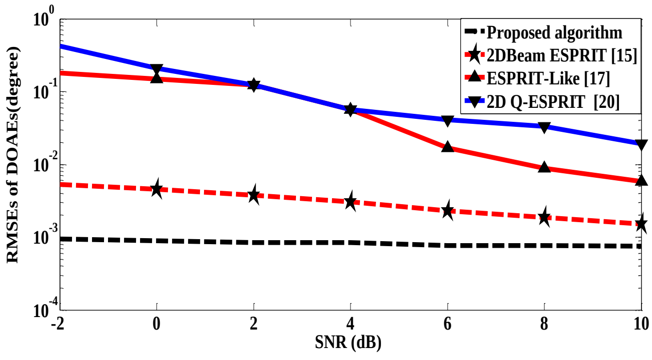

Fig. 7 RMSEs vs. SNR for T-ESPRIT with Doppler correction and Beam space-ESPRIT methods

Comparison results displayed in Fig.7 show that the proposed algorithm has a better performance, especially at a low SNR. This upgrade has been realized firstly due to the increase of DOAE accuracy when using the T-ESPRIT algorithm applying the subspace approach which decreases the errors caused by the model non linearity effect, secondly due to Doppler correction, which reduces the DOAE uncertainty associated with effect of the target movement. For more validation, a comparison between true and estimated angles (θ, φ) of two moving targets each with $v_s = 250\ m/sec$ is showed at Fig. 8 and Fig. 9 respectively. These comparisons highlight the meaning of glint error reduction and its importance.

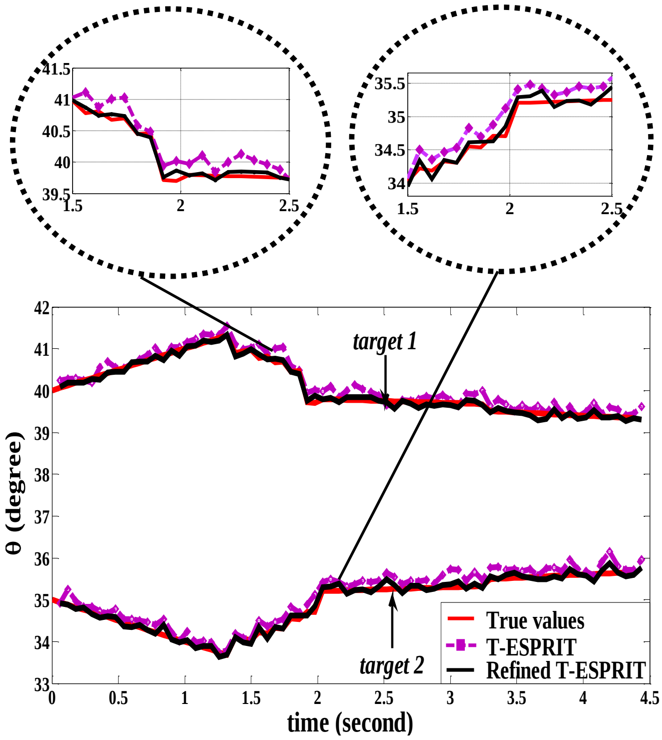

Fig. 8 The moving target elevation estimated angles

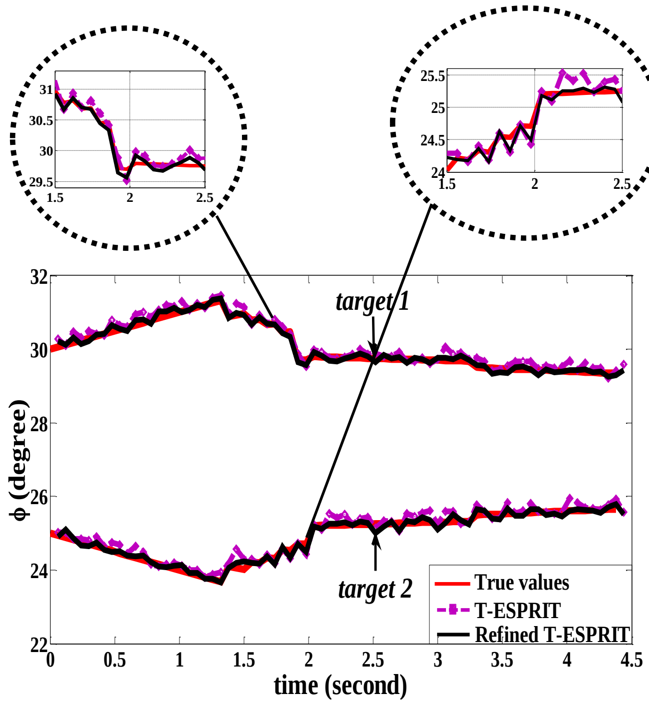

Fig. 9 The moving target azimuth estimated angles

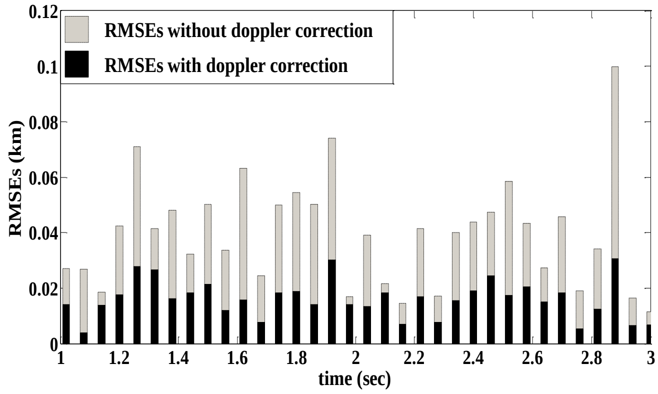

Fig. 10 The moving target RMSEs during the flight course

Clearly we can figure out that the proposed algorithm makes the estimated angles more close to the real angles which means reducing of angles errors (up to 0.15°- 0.3°) as shown in Fig. 8 and Fig. 9. This reduction in errors improves the radar resolution, which increases the targets separation ability within the TWS radar system (e.g. for radar has an angular resolution =0.75° this error reduction improves the separation ability about 20%). It also leads to more accurate correlation and association processes in the TWS radar system [24]. Additionally, Fig. 10 illustrates the importance of Doppler correction where it is noticed that the maximum RMSEs of the target estimated locations during the flight course without implementing the proposed Doppler correction reach about 100 meter, but the implementation of the proposed Doppler correction method reduces it that its maximum value reach about 30 meter. Thus, the proposed Doppler correction method reduces the errors about 70 %, which improves the performance of the TWS radar system. Results in table I indicate that the proposed algorithm requires $O(M+4r(IL)^2+8(IL)^3)$ flops [30], while the conventional ESPRIT algorithm needs $O(4d(IL)^2+ 8(IL)^3)$ flops. Also it notes from this table that the developed ESPRIT algorithm requires only about 9.7% of the computational time than required in the classical ESPRIT algorithm. Simply, we can say that the developed ESPRIT method achieved success into increasing the DOAE accuracy with low computational load, which leads to improve the estimator efficacy and TWS radar system performance.

V. CONCLUSIONS

In this paper, a new ESPRIT method has been developed based on the subspace processing technology and time series to the DOAE, which realizes a simultaneous parallel processing, and reduces the non-linearity effect in the model. Firstly, the T-ESPRIT method has been used to solve the 2D-DOAE. Secondly, the T-ESPRIT method has been refined with Doppler frequency to upgrade the estimation accuracy leading to improve the TWS radar system ability for targets separation by about 20%. It has been found that the estimation accuracy has been increased with low computational load; the computational time has been also reduced about 90%, which, consequently, enhances the estimator performance.

REFERENCES

[1] Youssef Fayad, Caiyun Wang, Qunsheng Cao Alaa El-Din Sayed Hafez, “A developed ESPRIT algorithm for DOA estimation,” *Frequenz*, vol.69, no. 3, pp. 263 – 269, 2015.

[2] Youssef Fayad, Caiyun Wang, Alaa El-Din Sayed Hafez, Qunsheng Cao, “Direction of Arrival Estimation Using Novel ESPRIT Method for Localization and Tracking Radar Systems,” Proceedings of the *IEEE 11th International Bhurban Conference on Applied Sciences & Technology (IBCAST)*, Islamabad, Pakistan, January 14–18, 2014, pp. 396-398.

[3] Nordkvist N. and Sanyal A.K.,“Attitude Feedback Tracking with Optimal Attitude State Estimation,” *American Control Conference*, 2010, pp.2861-2866.

[4] Xiaofei Zhang, Dazhuan Xu, “Improved coherent DOA stimation algorithm for uniform linear arrays,” *International Journal of Electronics*, vol. 96, no. 2, pp. 213-222, 2009.

[5] Renzheng Cao, Xiaofei Zhang, “Joint angle and Doppler frequency estimation of coherent targets in monostatic MIMO radar,” *International Journal of Electronics*, vol. 102, no. 5, pp. 792-814, 2015.

[6] Richard Roy and Thomas Kailath, “ESPRIT-Estimation of Signal Parameters Via Rotational Invariance Techniques,” *IEEE Transaction on acoustic, Speech, and signal processing*, vol. 37, no 7, pp. 984-995, 1989.

[7] Z. I. Khan, R.A. Awang, A. A. Sulaiman, M. H. Jusoh, N. H. Baba, M. MD. Kamal and N. I. Khan, “Performance Analysis for Estimation of Signal Parameters via Rotational Invariance Technique (ESPRIT) in estimating Direction of Arrival for linear array antenna,” *IEEE international RF And Microwave conference*, Kuala Lumpur, Malaysia, December 2-4, 2008.

[8] Aweke N. Lemma, Alle-Jan van der Veen and Ed F. Deprettere, “Joint Angle-Frequency Estimation using Multi-Resolution ESPRIT,” *Proceedings of the IEEE International Conference on Acoustics, Speech and Signal Processing*, 1998, vol.4, pp. 1957-1960.

[9] Gui-min Xu, Jian-guo Huang “Multi-resolution Parameters Estimation for Polarization Sensitivity Array,” *IEEE International Symposium on Knowledge Acquisition and Modeling Workshop, KAM*, 2008, pp. 180-183.

[10] Volodymyr Vasylyshyn, “Direction of Arrival Estimation using ESPRIT with Sparse Arrays,” *EUMA-6th European Radar Conference*, 30 September – 2 October, Rome, Italy, 2009.

[11] Aweke N. Lemma, Alle-Jan van der Veen and Ed F. Deprettere, “Multiresolution ESPRIT Algorithm,” *IEEE Transaction on signal processing*, vol. 47, no. 6, pp. 1722-1726, 1999.

[12] F. Gao, A. B. Gershman, “A generalized ESPRIT approach to direction of arrival estimation,” *IEEE Signal Processing Letters*,vol. 12, no. 3, pp. 254 – 257, 2005.

[13] Dang Xiaofang, Chen Baixiao, Yang Minglei, and Zheng Guimei, “Beamspace Unitary ESPRIT Algorithm for Angle Estimation in Bistatic MIMO Radar,” *International Journal of Antennas and Propagation*, http://dx.doi.org/10.1155/2015/621358.

[14] Wen Xu, Ying Jiang, Huiquan Zhang, “ESPRIT with multiple-angle subarray beamforming,” *EURASIP Journal on Advances in Signal Processing*. http://asp.eurasipjournals.com/content/2012/1/152, 2012.

[15] Cherian P. Mathews, Martin Haardt, Michal D. Zoltowski, “performance analysis of closed-form, ESPRIT based 2-D angle estimator for rectangular arrays,” *IEEE Signal Processing Letters,* vol. 3, no. 4, pp. 124 – 126, 1996.

[16] Y. Zhang, Z. Ye, X. Xu, and J. Cui, “Estimation of two-dimensional direction-of-arrival for uncorrelated and coherent signals with low complexity,” *IET Radar Sonar Navigation*, vol. 4, no.4, pp.507-519, 2010.

[17] Fang-Jiong Chen, Sam Kwong, Chi - Wah Kok, “ESPRIT-Like Two-Dimensional DOA Estimation for Coherent Signals,” *IEEE Transactions on Aerospace and Electronic Systems* vol. 46 , no. 3 , pp. 1477 – 1484, 2010.

[18] Jiang Hui, Yang Gang, “an improved algorithm of ESPRIT for signal DOA estimation,” *International conference on industrial control and electronics engineering*, Aug 23-25, 2012, pp.317 – 320.

[19] X. Xu, Z. Ye, “Two-dimensional direction of arrival estimation by exploiting the symmetric configuration of uniform rectangular array,” *IET Radar Sonar Navigation*, vol. 6, no.5, pp.307-313, 2012.

[20] Yang Li, Jian Qiu ZHANG, and Bo HU ZHOU, “A novel 2-D quaternion ESPRIT for joint DOA and polarization estimation with crossed-dipole arrays,” *IEEE International Conference on Industrial Technology (ICIT),* Cape Town, Feb 25-28, 2013, pp.1038 - 1043.

[21] Fawaz Alassery, Walid K. M. Ahmed, Mohsen Sarraf, and Victor Lawrence, “A Low Computational Complexity Statistical Discrimination Algorithm for Collision Detection in Wireless Sensor

Networks," *IAENG International Journal of Computer Science*, vol. 41, no.3, pp.204-211, 2014.
[22] Weiya Yue, John Franco, "A New Way to Reduce Computing in Navigation Algorithm", *Engineering Letters*, vol.18, no.4, pp.341-350, 2010.
[23] Christian Wolff, Radar Basics, http://www.radartutorial.eu., 2015.
[24] Bassem R. Mahfaza, "Radar Systems Analysis and Design Using MATLAB, " *Chapman & Hall/CRC*, 2000.
[25] F. B. BERGER, "The Nature of Doppler Velocity Measurement," *IRE transactions on aeronautical and navigational electronics*, vol. ANE-4, no. 3, pp. 103 – 112, 1957.
[26] A. Nabavizadeh, M. W. Urban, R. R. Kinnick, and M. Fatemi, "Velocity Measurement by Vibro-Acoustic Doppler," *IEEE Transactions on Ultrasonics, Ferroelectrics, and Frequency Control*, vol. 59, no. 4, pp. 752 - 765 , 2012.
[27] A-level Physics (Advancing Physics), http://en.wikibooks.org ,2015.
[28] Aldo N. D Andrea, Umberto Mengali and Ruggero Reggiannini, "The Modified Cramer-Rao Bound and its Application to Synchronization Problems," *IEEE Transaction on communication*, vol. 42, no. 2, pp. 1391- 1399, 1994.
[29] Steven Thomas Smith, "Statistical Resolution Limits and the Complexified Cramér–Rao Bound," *IEEE Transaction on signal processing*, vol. 53, no. 5, pp. 1597-1609, May. 2005.
[30] Cheng Qian, Lei Huang and H.C. So "Computationally efficient ESPRIT algorithm for direction-of-arrival estimation based on Nyström method," Signal Processing, vol. 94, pp.74-80, 2014.

Youssef Fayad (Alexandria Egypt, 4/9/1975) received the B.S. In electronic engineering and the M.S. in communications and electronics from faculty of engineering, Alexandria University, Egypt, in 1997, 2010 respectively. He is currently in Ph.D. degree in radar system in Nanjing University of Aeronautics and Astronautics, college of electronic and information engineering, Nanjing, china. He is an IAENG Member, and a Student Member of IEEE, he is also worked as an Assistant Lecturer in Air Defense College, Egypt. Mr. Fayad research interests in antenna and radar signal processing.

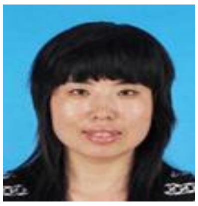

Caiyun Wang was born in Shanxi, China, on September 30, 1975. She graduated in 1996 with a B.S. degree and in 1999 with a M.S. degree. She received the Ph.D. degree in signal and information processing from Beihang University, Beijing, China, in 2008. She is currently an associate professor with the College of Astronautics , Nanjing University of Aeronautics and Astronautics (NUAA). Her major research interests are in the fields of radar automatic target recognition (RATA), radar signal processing, and adaptive signal processing, and pattern recognition.

Qunsheng Cao received his Ph.D. in electrical engineering from The Hong Kong Polytechnic University in 2001. From 2001 to 2005 he worked as a Research Associate in the Department of Electrical Engineering, University of Illinois at Urbana-Champaign and at the Army High Performance Computing Research Center (AHPCRC), University of Minnesota. In2006, Dr. Cao joined the Nanjing University of Aeronautics and Astronautics (NUAA), China, as a Professor of electrical engineering. Dr.Cao's current research interests are in computational electromagnetics, antenna and microwave technology and the radar signal processing. Dr. Cao has published more than 120 academic papers in refereed journals and conference proceedings.